



## Article

# Magnetic Separation and Enrichment of Fe–Ti Oxides from Iron Titaniferous Beach Sands: Process Design Applied to Coastal Ecuador

Willam Trujillo <sup>1</sup>, Joseph Cobo <sup>1,2</sup>, Dayanna Vera-Cedeño <sup>1</sup>, Alex Palma-Cando <sup>1</sup>, Jorge Toro-Álava <sup>3</sup>, Alfredo Viloria <sup>1</sup> and Marvin Ricaurte <sup>1,\*</sup>

- <sup>1</sup> Grupo de Investigación Aplicada en Materiales y Procesos (GIAMP), School of Chemical Sciences and Engineering, Yachay Tech University, Hda. San José s/n y Proyecto Yachay, Urcuquí 100119, Ecuador
- <sup>2</sup> École Nationale Supérieure en Génie des Technologies Industrielles (ENGSTI), Université de Pau et des Pays de l'Adour, 64000 Pau, France
- <sup>3</sup> Grupo de Investigación Aplicada en Materiales y Procesos (GIAMP), School of Earth, Energy and Environmental Sciences, Yachay Tech University, Hda. San José s/n y Proyecto Yachay, Urcuquí 100119, Ecuador
- \* Correspondence: mricaurte@yachaytech.edu.ec

**Abstract:** Iron titaniferous sands, also called black sands, are a source of various magnetic minerals, such as iron and titanium (Fe–Ti) oxides, with countless scientific and industrial applications. Ecuador is deemed a geo-diverse country that contains deposits of black sands in the Andean and coastal regions; therefore, the industrialization of these magnetic sands might be of high interest. This study presents a preliminary industrial design for the magnetic separation process of Fe–Ti oxides from iron titaniferous Ecuadorian beach sands. Four stages are considered for the process, involving collecting, drying, screening, and magnetic separation. This proposal returns the large particles (>150 µm) and the non-magnetic fraction to the original place, generating a minimum environmental impact with the support of natural marine and coastal processes. The process design criteria are based on engineering guidelines, sampling, and characterization of eleven black sand samples. Using conventional techniques, the water content, granulometric distribution, particle size, and semi-quantitative Fe–Ti oxide concentration were determined for the different sand samples. It is estimated that Fe–Ti oxide production may reach 5.835 metric tons per day (5.835 mtpd) with a magnetic content of 97.50%, starting from 100 mtpd of black sands. Based on an economic analysis (Class V), a net profit of USD 835,875.63 is expected during the first year of production. Thus, the magnetic separation and enrichment of Fe–Ti oxides from iron titaniferous coastal sands exploitation should allow the commercial valorization of these resources in an eco-friendly way, i.e., with economic benefits and minimization of environmental impact in the source area.

**Keywords:** magnetic separation; iron and titanium oxides; black sand; ilmenite; process design; beach sand; Ecuador



**Citation:** Trujillo, W.; Cobo, J.; Vera-Cedeño, D.; Palma-Cando, A.; Toro-Álava, J.; Viloria, A.; Ricaurte, M. Magnetic Separation and Enrichment of Fe–Ti Oxides from Iron Titaniferous Beach Sands: Process Design Applied to Coastal Ecuador. *Resources* **2022**, *11*, 121. <https://doi.org/10.3390/resources11120121>

Academic Editors: Gregory Poelzer, Katharina Gugerell and Andreas Endl

Received: 5 August 2022

Accepted: 17 October 2022

Published: 14 December 2022

**Publisher's Note:** MDPI stays neutral with regard to jurisdictional claims in published maps and institutional affiliations.



**Copyright:** © 2022 by the authors. Licensee MDPI, Basel, Switzerland. This article is an open access article distributed under the terms and conditions of the Creative Commons Attribution (CC BY) license (<https://creativecommons.org/licenses/by/4.0/>).

## 1. Introduction

Iron titaniferous sands are natural mixtures of minerals that contain a high percentage of iron and titanium (Fe–Ti) oxides with traces of aluminum and zirconium oxides, among others [1]. Usually, these minerals are magnetite (Fe<sub>3</sub>O<sub>4</sub>), ilmenite (FeTiO<sub>3</sub>), hematite (Fe<sub>2</sub>O<sub>3</sub>), rutile (TiO<sub>2</sub>), zircon (ZrSiO<sub>4</sub>), and silicates, such as quartz (SiO<sub>2</sub>) [2]. Due to the predominance of very dark-colored materials, they are also named “black sands”. Iron titaniferous sands originated from strongly eroded volcanic rocks. The materials resulting from erosion are transported, forming sediments by the mechanical action of water. The specific density differences between iron titaniferous phases from other materials subjected to the mechanical action of the river and sea waters cause their accumulation on the

beaches [3]. Iron titaniferous sands can be found in several regions worldwide, including Ecuador, specifically on the maritime coastline, forming exotic black sand beaches [4].

Fe–Ti oxides are used as raw materials in several industries for different purposes and applications [1]. For example, titanium dioxide can be used to produce paintings, paper, rubber, plastics, ceramics, surgical instruments, aircraft parts, coating for welding, and as a raw material for titanium metal production [5]. Moreover, producing metallic iron and titanium starting from these Fe–Ti oxides may trigger countless industrial applications in the automobile, construction, and steel industries [6,7]. Therefore, separating Fe–Ti oxides from iron titaniferous sands represents an essential process for producing final value-added products. Magnetic separation has been applied in ore processing to separate magnetic materials, such as iron oxides, from the bulk of non-magnetic minerals with smaller specific densities [8]. This approach separates particles by passing finely ground ore particles through a magnetic field at different intensities. The result is the retention of paramagnetic particles on the magnetic separator, depending upon the magnetic susceptibility of minerals. At the same time, non-magnetic or diamagnetic components deflect and fall off the apparatus.

This study aims to develop a preliminary industrial design of a magnetic separation process of Fe–Ti oxides from iron titaniferous beach sands. It proposes a case study for the coast of Ecuador. The process stages are detailed, providing information on some characteristics of the magnetic separation equipment. The plant capacity is estimated based on technical and economic criteria. The characterization of the raw material in the case study is also presented. This magnetic separation proposal returns the non-magnetic material to its original place. It should generate a minimum impact on the environment because it is conceived as a part of non-destructive and non-aggressive natural processes that guarantee the return of the non-magnetic materials to the source area, thus maintaining the natural physical and biological conditions.

## 2. Process Design Proposal

The process consists of the following four stages [9–11]: collecting, drying, screening, and magnetic separation, as shown in Figure 1.

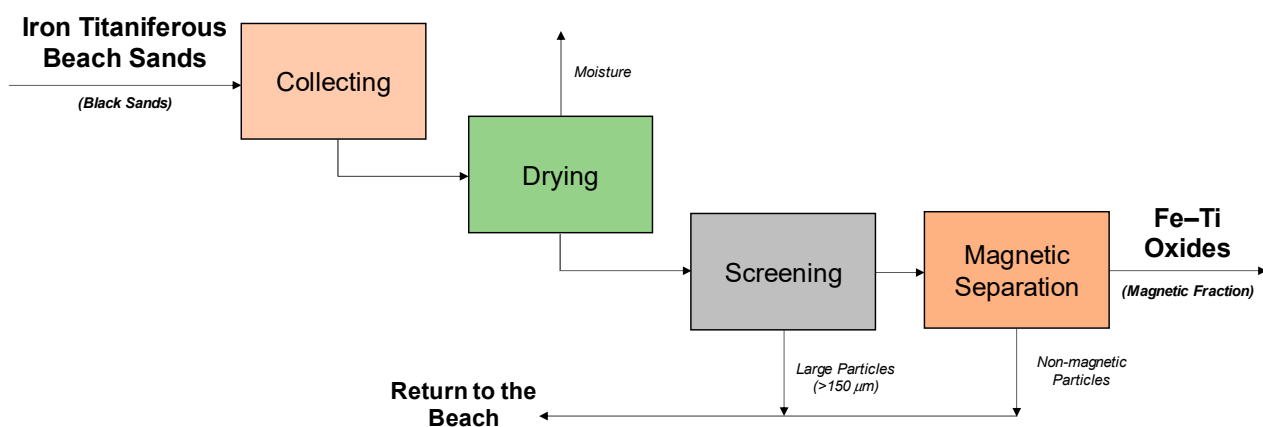


Figure 1. Block diagram (BD).

- **Collecting stage:** This stage is carried out through a backhoe in charge of managing the raw material. The sand extraction in coastal regions is low risk to the local environment because the waves, tides, and winds will help compensate the exploited area with sandy sediments by natural filling. Fragments of light minerals and lithics may be reworked by the backwashing process and transported down the beach zone to a water depth between the lower tide zone to the upper shoreface zone, which can be conducted by littoral drift around the shoreline promontory. This phenomenon is known as coastal drift, which transports sediments along the coast due to the wave's movement [12]. In contrast, some heavy minerals (such as iron titaniferous sands) are

trapped at the berm on the up-current side of the beach. Over time, the heavy mineral load is increased on the cape's up-current side [13]. In addition, the non-magnetic fraction is returned to the extraction site after the magnetic separation. Considering operational flexibility, high reliability, easy availability, and economic feasibility, the cyclical operational method of excavation–unloading–excavation should be performed by excavators or backhoes, with or without auxiliary means of transport (pipelines, conveyor belts, or dump trucks) [14].

- **Drying stage:** The drying operation eliminates the humidity in a solid by thermal means. The sand's moisture may represent a certain degree of cohesion between the solid particles, making the mechanical and magnetic separation processes challenging [15]. Rotary dryers are commonly considered to carry out the drying process [13]. In the proposed design process, the heat is transferred directly by hot air or a mixture of combustion gases that flow countercurrent through the cylindrical vessel, where the sand sample will be placed and then dried. The dry time and temperature depend on the mass of the sand that enters the system and the moisture content [16]. It is recommended to place a trashrack (mesh size: 1 cm) at the entrance of the dryer to retain the large solids (rocks, solid wastes, seashells, organic remains, etc.) that could be found in the sands.
- **Screening stage:** Sieving consists of passing the sands through a jigger that contains sieves of different sizes [17]. The progressively smaller mesh size produces a more suitable raw material for the magnetic separation process. Abdel-Karim et al. [18] screened black sands from Egypt and found a selective concentration of magnetic particles in grain sizes between 63  $\mu\text{m}$  and 250  $\mu\text{m}$ . Similar results were obtained using black sands from Colombia [19,20], Greece [21], Indonesia [22], Malaysia [23,24], Turkey [25], and some African countries [26]. Therefore, the screening can be considered as a pre-enrichment stage of the magnetic fraction in iron titaniferous sands. Grain size distribution analysis is necessary to determine the range where magnetic particles are concentrated in black sands [27,28], as was performed in this study.
- **Magnetic separation stage:** Regarding the magnetic separation process, materials can be classified into two large groups –paramagnetic and diamagnetic– depending on whether they are attracted or repelled by a magnet. Paramagnetic materials are drawn along the lines of magnetic force towards regions of higher field intensity. The diamagnets are repelled when an external magnetic field is applied to the point where the field strength is already very low. Diamagnetic substances cannot be concentrated magnetically. The equipment used as magnetic separators consists of magnetic fields generated either by electricity or natural magnetic materials [9]. All materials on Earth display certain magnetic properties in the presence of an external magnetic field [29]. Thus, magnetic separators aim to take advantage of the difference in minerals' magnetic properties to separate paramagnetic Fe–Ti oxides from diamagnetic oxides in the black sands [30,31]. The magnetic intensity depends on the minerals to be separated [32]. Ilmenite –a paramagnetic mineral– is one of the high-value minerals that predominate in black sands [2]. The values of the magnetic susceptibility vary from  $0.2 \times 10^{-6} \text{ m}^3/\text{kg}$  to  $1.5 \times 10^{-6} \text{ m}^3/\text{kg}$  for ilmenite [22,29]. Due to efficiency parameters, it is essential to consider that the magnetic separators are usually used for a grain size of  $<150 \mu\text{m}$  because it allows for a cleaner final product, avoiding unnecessary loss of valuable material [9]. The magnetic separators are divided into dry and wet magnetic separators [33]. Dry magnetic separation is a technique that dates back to the beginning of the last century. It has successfully been practiced to remove tramp iron from process streams, beneficiating strongly magnetic and feebly magnetic minerals, such as wolframite, cassiterite, or ilmenite [34]. Purification of numerous industrial minerals, such as andalusite, glass sand, fluorspar, feldspar, diamonds, and others, is often carried out dryly by removing fine, strongly magnetic impurities. Developed eddy-current separators operate in a dry mode [9]. On the other hand, two types of wet magnetic separators are frequently used, including drum separators with

permanent magnets or electromagnets and magnetic filters [35]. Wet drum separators are a type of equipment that is used as recovery units in dense media plants for the concentration of ferromagnetic iron minerals, and magnetic filters are used to eliminate or separate fine ferromagnetic particles from liquids or liquid suspensions [9].

Moreover, an additional step involves returning the large particles (>150  $\mu\text{m}$ ) and the non-magnetic fraction of the processed beach sands to the source area. The magnetic separation process design is expected to have a minimum impact on the coastal environment. Once returned to the source area, the sands will be redistributed, first employing excavators or backhoes, and then naturally rearranged and modeled by the wave and tide marine processes that act on the beach zone.

### 3. Process Design Applied to Coastal Ecuador

#### 3.1. Iron Titaniferous Sands in Ecuador

Ecuador is considered a geo-diverse country [36], composed of, from west to east, an oceanic ridge, coastal plain, accreted oceanic plate, island arc, continental arc, and metamorphic and granitic substratum, overlain by sedimentary basins and volcanoclastic deposits [37]. The black sands appear as heavy-mineral sand deposits on the Ecuadorian shoreline [38]. In the country, Fe–Ti oxides are mainly used in Portland cement production [39,40] and the steel industry for steel production [41]. The cement industry is associated with the construction sector, one of the most dynamic sectors in the Ecuadorian economy. The Central Bank of Ecuador estimates that the construction sector represented 7.22% of the gross domestic product (GDP) in 2021 [42]. In addition, Fe–Ti oxides may be used in the oil and gas industry for natural gas sweetening [43,44] or within the textile industry to perform adsorption and photocatalytic processes to remove textile dyes from textile effluents [45]. The Ecuadorian textile industry is the second largest employment generator in the country and represented 7.5% of the entire manufacturing sector in Ecuador until 2015 [46]. Moreover, the textile industry represented, on average, 0.77% of the domestic GDP between 2016 and 2020 [47].

Considering the different uses of Fe–Ti oxides in the country, iron titaniferous sands can be used on a large scale to supply the internal demand. However, to the best of our knowledge, no studies on industrial magnetic separation processes for iron titaniferous sands have been reported in Ecuador [48].

#### 3.2. Iron Titaniferous Sand Sampling and Characterization

In this study, eleven sites with black sand occurrences from the coastal zone of Ecuador (Figure 2) were selected as the potential areas of raw materials for magnetic separation process development. Table 1 shows the identification and geographical location (province and GMS coordinates) of sandy samples taken from different zones in Ecuador.

**Table 1.** Identification and geographical location of black sand samples from Ecuador.

Samples	Sampling Zone (Province)	Location (GMS Coordinates)
SYA-103	Anconcito beach * (Santa Elena)	2°16'23.77" S–80°55'23.96" W
SYA-104	Anconcito beach * (Santa Elena)	2°16'23.30" S–80°55'23.22" W
SYO-105	Olón beach * (Santa Elena)	1°48'46.54" S–80°45'24.78" W
SYM-106	North of Montañita * beach (Santa Elena)	1°53'59.67" S–80°45'26.21" W
SEV-201	Río Verde * (Esmeraldas)	1°4'34.55" N–79°24'49.98" W
SET-202	Tonsupa * (Esmeraldas)	0°53'32.29" N–79°48'52.29" W
SET-203	Tonsupa * (Esmeraldas)	0°53'32.50" N–79°48'53.22" W
SMP-204	Pedernales * (Manabí)	0°4'53.20" N–80°3'18.14" W
SEM-205	Mompiche * (Esmeraldas)	0°30'37.72" N–80°1'11.61" W
SEM-206	Mompiche ** (Esmeraldas)	0°30'35.29" N–80°1'12.50" W
SEG-207	Punta Galera *** (Esmeraldas)	0°49'6.80" N–80°2'54.86" W

\* From the upper part of the shoreline (high tide). \*\* Close to the river mouth of a mini funnel-shaped sandy estuary. \*\*\* Close to the coastal inlet.



**Figure 2.** Location of sampling sites on the map of Ecuador.

The sampling process involved digging a 50–60 cm deep hole to take the sample from the entire edge. Figure 3 shows the physical appearance of black sands and their petrographic description (P.D). In general, most quartz-rich sandy samples included in this study were gray to pale gray and deep gray in color; ranging from medium-grained to very fine-grained in size; subrounded to subangular; good to moderately sorted; and composed of quartz, multi-color fragments of clasts, complemented with some fragments of bivalves and gastropods, and with low content of subhedral to anhedral black magnetite and metallic minerals. Only one sandy sample (SMP-204) was quartz-rich, coarse-grained, subrounded, and poorly sorted, with fragments of clasts and bivalves. The black sands, on average, are classified as sub-lithoarenites rich in chert (composed of silicon oxide) and quartz, with similar hardness (7 on the Mohs scale), which guarantees the clean mechanical enrichment of sandy sediments, with limited presence of weathering products and few silty to clayey residues.

Approximately 9 kg of each sample was stored on-site in plastic bottles. Then, laboratory analyses were carried out, such as water content by moisture loss, granulometric distribution by sieving of sands, particle size by dynamic light scattering (DLS), and semi-quantitative Fe–Ti oxide concentration by energy dispersive spectroscopy (EDS) on a scanning electron microscope (SEM). The methodology details used in each laboratory analysis are available in the Supplementary Material.

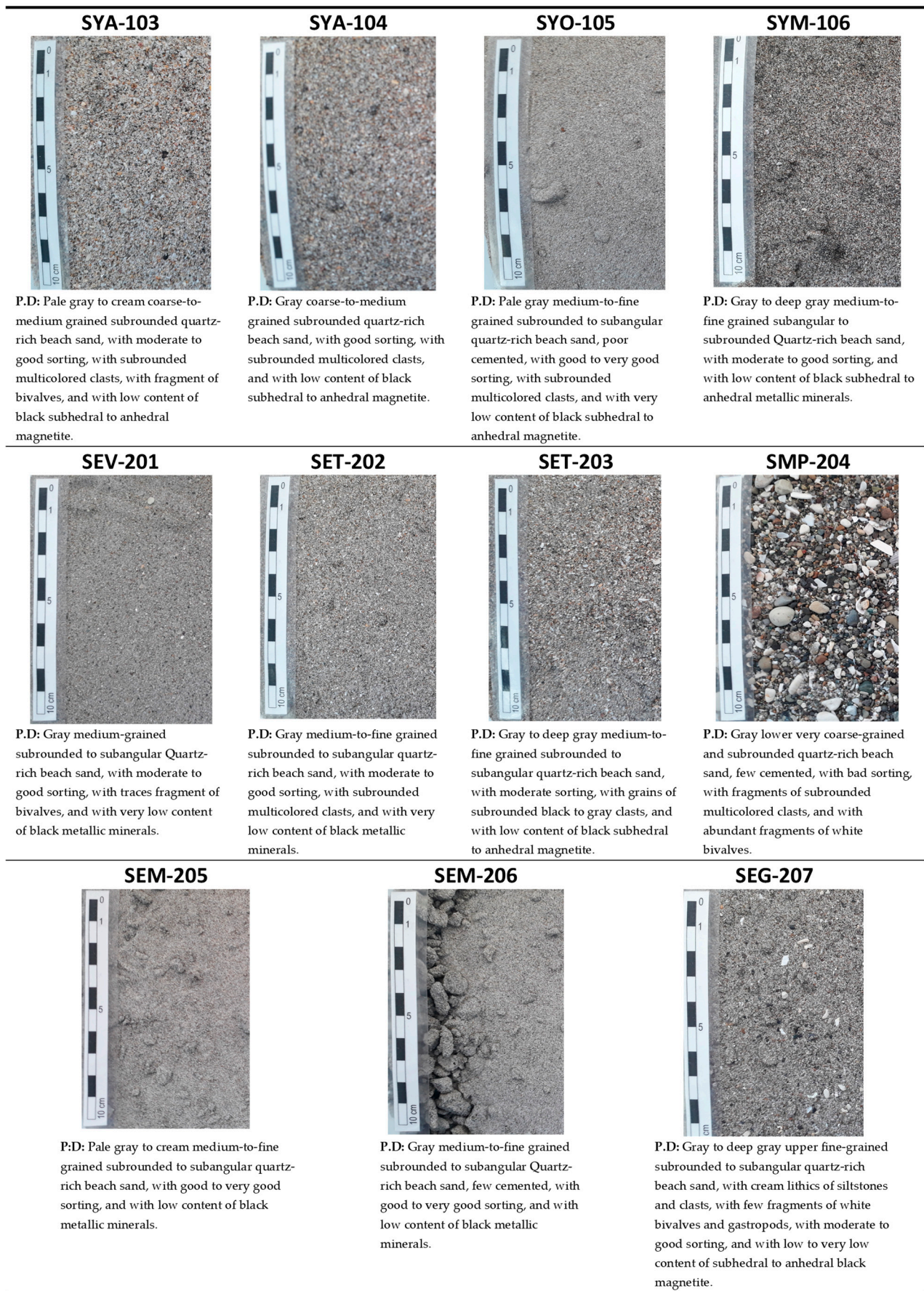


Figure 3. The physical appearance of black sand samples and their petrographic description.

The percentage of water content in the iron titaniferous sands analyzed in this study is presented in Figure S1. A median water content value of 15.24% justifies a drying stage before the screening. In addition, Figures S2 and S3 and Table S1 show the results of the granulometric size distribution. A median grain size of 310  $\mu\text{m}$  on average, obtained through sieving analysis, represents the significant range of grain sizes of these sandy beach samples from which the iron-rich metallic minerals were extracted. The average grain size of approximately 85  $\mu\text{m}$  for the iron titaniferous minerals led us to employ only the fraction comprised of very fine-grained sands with coarse-grained silts of minimum grain sizes for the extraction phase of black metallic minerals. An average proportion of gravels, sands, and fine particles of 1.5%, 98%, and 0.5%, respectively, shows that the black sand samples under investigation are mainly classified as sands [38,49]. Figure S3 relates two granulometric parameters, the uniformity coefficient (CU) versus the mean size of sandy particles ( $d_{50}$ ). In general, the uniformity coefficient indicates the range of grain sizes present in a given sandy sample. It is defined as  $CU = d_{60}/d_{10}$ , where  $d_{60}$  and  $d_{10}$  represent the grain diameter that corresponds to 60% and 10% passing, respectively [50]. A large CU value indicates the presence of different grain sizes; on the contrary, a small CU value indicates that most grain sizes are concentrated in a small range of sizes. In addition, the cross-plot in Figure S3 shows a narrow interval of CU ( $1.45 \leq CU \leq 2.50$ ) for all the grain sizes ( $0.23 \leq d_{50} \leq 0.42$ ), proving a uniform and narrow granulometric distribution of the eleven beach sands analyzed, with very few gravel sizes and very few silty to clayey sizes. These CU and  $d_{50}$  values are an industrial advantage for separating the grain fractions both magnetically and physically.

Table S2 shows the semi-quantitative analysis of natural sands expressed as oxides. This analysis revealed considerable Fe–Ti oxides content in the samples SYA-104, SEV-201, SMP-204, and SEM-205. The highest content of iron oxides is found in SYA-104 (6.91%), while the highest titanium content is in sample SEM-205 (1.56%). Hence, the sands with the highest iron and titanium content may be suitable potential candidates for the magnetic separation process. The behavior and properties of particulate materials depend upon morphology, particle size, and particle size distribution [51]. The magnetic separation was carried out using a plastic-covered magnet (2 Tesla) (see Figure S4). On average, the percentage of magnetic particles of sand is 8–10 wt.%. Iglesias et al. [44] showed, by DRX analysis, that the content of magnetite and ilmenite in magnetic-enriched sand samples was higher than 85.0%.

### 3.3. Raw Material Location and Plant Capacity

Since Ecuador is a geo-diverse country, iron titaniferous sands are found in several provinces across the country. Based on the Fe–Ti oxide concentration in the black sands, the following four black sand samples in Ecuador may be considered as raw material sources (see Figure 2): (1) SYA-104 in Anconcito (Santa Elena province), (2) SEV-201 in Río Verde (Esmeraldas province), (3) SMP-204 in Pedernales (Manabí province), and (4) SEM-205 in Mompiche (Esmeraldas province).

The plant's processing capacity is 100 metric tons of black sand per day (100 mtpd). It is established based on a market study, considering the following main criteria: the selection of raw material, process stages, domestic and international demand for the Fe–Ti oxides, and economic analysis (Class V). In this study, an overall yield of 5.045 tons of Fe–Ti oxides is considered for 100 mtpd of feed.

### 3.4. Process Design Criteria

Table 2 shows the process design criteria used in this study. Technical parameters are established for the screening, drying, and magnetic separation stages based on engineering criteria and the best practices commonly used in this type of equipment, in terms of efficiency and loss percentages. At the laboratory scale, the magnetic enrichment of metallic oxides was successfully demonstrated by using a magnetic separator, e.g., a permanent magnet [44].

**Table 2.** Process design criteria.

Stages			References
Input			
Feed	100 mtpd		(This study)
Water content	20 wt.%		
Dry magnetic fraction	10 wt.%		
Overall magnetic fraction	8 wt.%		
Drying			
Efficiency	90%		[15,52–55]
Sand loss	1%		
M-NM distribution	3%		
Screening			
Efficiency	70%		[56–58]
Sand loss	10%		
M-NM distribution	5%		
Magnetic Separation			
Separation	90%		[9,33–35,53,59,60]
Distribution M-NM	95%		
Magnet efficiency	70%		

Note: M-NM: magnetic–non-magnetic distribution.

### 3.5. Detailed Process Description

Figure 4 shows the process flow diagram (PFD). The magnetic separation process from the raw material input to the Fe–Ti oxide concentrates as the final products is shown in detail. First, it is crucial to define the tags used for stage identification, which are as follows: B-101 (collector), T-101 (dryer), F-101 (screen), F-102 (magnetic separator), and H-101, H-102, and H-103 are used for the conveyor belts that transport the solid material from one stage to another. The magnetic separation process starts at B-101, and the sand (#1) is stored, before being transported by H-101 to the dryer T-101. Two outputs from T-101 are the dried sand (#2) that are further transported by H-103 to the screen F-101 and the waste from the drying process (#5). Then, the two output fluxes from F-101 refer to screened sand (#3), which H-103 transports to the magnetic separator F-102 and the waste from the screening process (#6). Finally, the outputs from F-102 are the Fe–Ti oxides (#4) and the non-magnetic fraction (#7). It is estimated that Fe–Ti oxides are produced at 5.835 mtpd, with a magnetic content of 97.50% and low moisture.

The large particles and the non-magnetic fraction, which correspond to 75.365 mtpd, are returned and redistributed to the beach again. These sub-products represent 91.71% of the black sand fed to the process, expressed on a dry basis. As mentioned above, the return and redistribution of large particles and the non-magnetic fraction is expected to minimize the environmental impact on the source area. Afterward, the waves, tides, and other marine processes will progressively rearrange the material. The black sand exploitation proposal is based on physical processes that involve drying, screening, and magnetic separation, avoiding using additives or chemical compounds that may negatively impact the coastal zone.

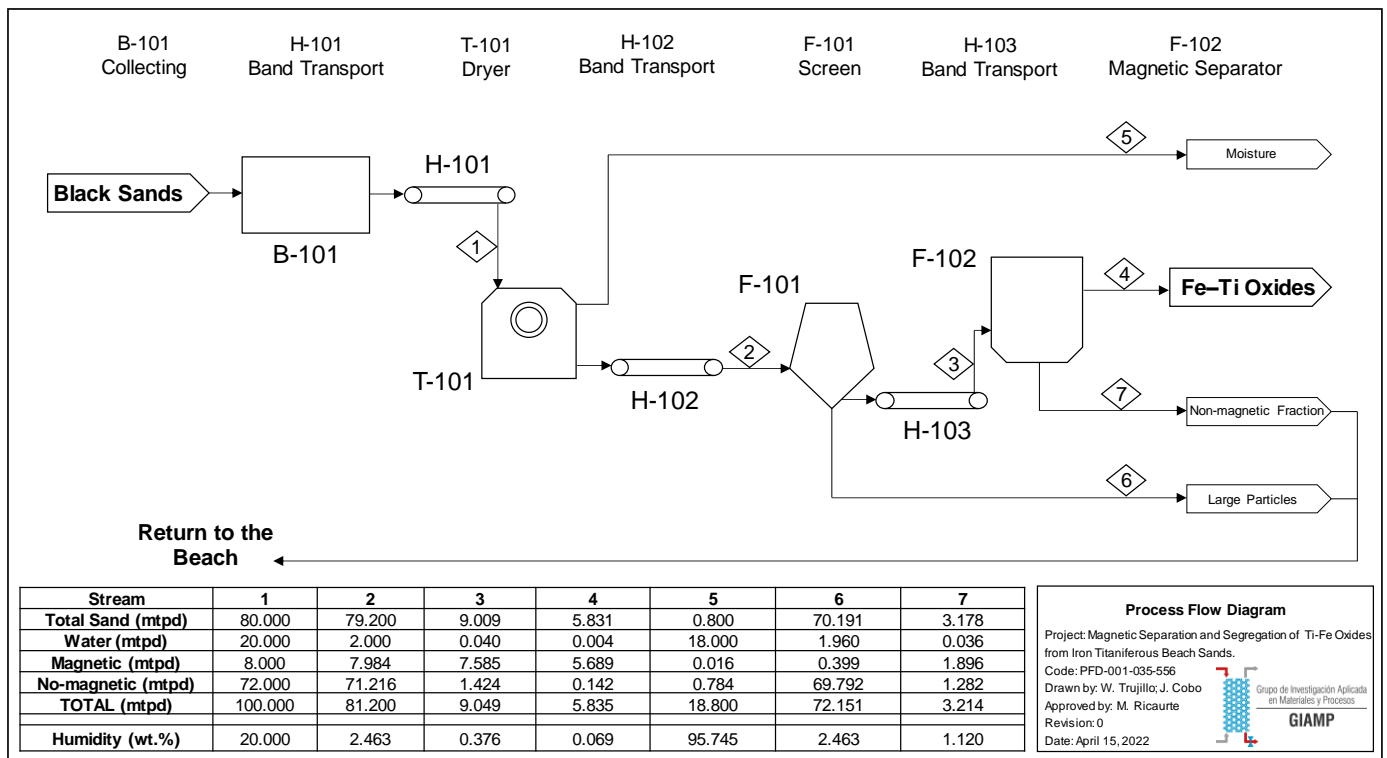


**Figure 4.** Process flow diagram (PFD).

### 3.6. Technology Selection

The magnetic separation process consists of the following four main stages:

- **Collecting:** Generally, the backhoes excavate at a depth of 4.83 m. The bucket has a volume of 0.8 m<sup>3</sup> and a capacity of approx. 97 kg [61].
- **Drying:** Rotary dryers are essential and valuable in various industrial process settings [54]. Their typical dimensions are 2.74 m (9 ft) in diameter and 13.72 m (45 ft) in length. In direct-heat revolving rotary driers, hot air or a mixture of flue gases and air flows countercurrent through the cylinder. The feed rate, the speed of rotation or agitation, the volume of heated air or gases, and their temperature depend on the input physical characteristic to reach the desired output quality. Hence, the solid is dried just before discharge [55].
- **Screening:** There are several industrial sieve models, but the most suitable has a production capacity of up to 3000 kg/h. This equipment is made of stainless steel, and the diameters are around 600 to 800 mm [58].
- **Magnetic separation:** In dry magnetic separation, the most common equipment is drum separators with permanent magnets or electromagnets and magnetic filters [9]. The efficiency of drum magnetic separators at the industrial level varies from 60% to 90% [60].

### 3.7. Economic Analysis (Class V)

Sand has become the second most consumed raw material globally after water [62] and is one of the most lucrative businesses [63]. A study by the United Nations, presented in Geneva in 2019, shows that the demand for sand and gravel is around 50,000 million tons annually. This scenario is three times greater than twenty years ago [64]. The black sand price is linked to the national or international market based on Fe purity. The 62% purity iron ore benchmark proposed to China was, on average, USD 121.50 per ton in 2014, according to a Reuters poll of 14 analysts [65]. The following statement should also be noted: "After 2014, due to the newly increased output of iron ore put into operation by

the global mining enterprises in 2014–2015, the supply of iron ore will be oversupplied. Iron ore prices fell for 4 consecutive years, until 2016; however, from 2016, it reversed again” [66].

The reference price of sand per metric ton in the last five years has an interest rate increase of 207.06%. In 2015, the production of 1 ton of raw material for Minagrotec, an Ecuadorian company dedicated to the extraction of this raw material, cost USD 27.75 per ton. It is important to indicate that the national market price in 2015 was USD 33.27 per ton. The national demand for these sands in 2014 was 512 tons per month, and in the international market, the request was 1008 tons per month [67].

Engineers seek solutions to problems, and the economic viability of each potential solution is usually considered, along with the technical aspects. Fundamentally, engineering economics involves formulating, estimating, and evaluating economic outcomes when alternatives are available to accomplish a defined purpose [68]. Industrial processes start whenever they present a favorable economic aspect, and expenses and profits must be analyzed before carrying out any process, project, or investment. There are two types of expenses, direct and indirect. The direct expenses correspond to raw materials, labor, equipment, and machinery. On the other hand, the indirect costs correspond to administrative staff salaries and product distribution costs. Furthermore, it is crucial to mention the net profit, which corresponds to the total income obtained, minus all the expenses incurred during the process [69]. The demand for Fe–Ti oxides, both nationally and internationally, grows, for which monthly production of 2000 tons of treated sand has been taken as a reference.

The initial investment includes the permanent opening of an office in a leased premise to sample the sand selected for extraction and the heavy machinery used in production, tools, employees, and services to be used in the project. Table 3 shows the economic analysis for the following years. The initial investment was estimated at USD 163,077.

**Table 3.** Economic analysis balance sheet.

Years	2022	2023	2024	2025
Inflation rate	2.32%	1.38%	1%	1%
Initial investment (USD)	163,077			
Operational costs	Annual cost	Annual cost	Annual cost	Annual cost
Salaries of operating personnel (USD)	118,048.49	118,048.49	118,048.49	118,048.49
Supplies (USD)	28,104.00	28,456.58	28,741.14	29,028.55
Basic services (USD)	9000.00	9000.00	9000.00	9000.00
Operational maintenance (USD)	68,000.00	68,000.00	68,000.00	68,000.00
Total operational costs (USD)	283,152.49	283,505.07	283,789.63	284,077.04
Total income for sale (USD)	2,099,430.00	2,099,430.00	2,099,430.00	2,099,430.00
Gross profit (USD)	1,816,277.51	1,815,924.93	1,815,640.37	1,815,352.96
Taxes (USD)	817,324.88	817,166.22	817,038.17	816,908.83
Net profit (USD)	835,875.63	998,758.71	998,602.20	998,444.13

The maintenance of the plant is carried out in the winter months (April–May), since they can affect the efficiency of the equipment in the screening and drying stage, and thus affect the overall process. Maintenance costs were estimated at USD 68,000 per year. The taxes treated in the Ecuadorian public policy for the mining sector were estimated at 45% of the gross profit [7].

In the first year, maintaining the upward trend in the price of iron and titanium ore and discounting the initial investment, a net profit of USD 835,875.63 is expected. The analysis states that after treating and selling the product of 3272.78 tons of iron titaniferous sands, the plant will start to make a profit.

#### 4. Summary and Conclusions

This study has established a preliminary efficient and sustainable design for a magnetic separation process of iron titaniferous beach sands. The industrial process involves the following four stages for mineral separation: collecting, drying, screening, and magnetic separation. The sand collection on coastal beach zones is performed using a backhoe, which is responsible for carrying these sands into the collection center. The drying stage is required because of the humidity percentage, which causes a certain degree of cohesion in the sands, making the magnetic separation less efficient. The screening process removes impurities, such as solid and organic residues, in the raw sand and reduces the sand particle size. Finally, the magnetic separation stage splits the magnetic fraction, enriched with Fe–Ti oxides, from the non-magnetic fraction. Considering a case study in Ecuador, eleven sandy samples from different locations in the coastal zone of Ecuador were sampled, stored, and then characterized. The laboratory analysis determined each sandy sample's water content, granulometric distribution, particle size, and the semi-quantitative Fe–Ti oxide concentration. Based on the experimental data, SYA-104, SEV-201, SMP-204, and SEM-205 can be considered as raw materials for the industrial magnetic separation process. The characterization results and technical and economic criteria were in line with the plant's capacity and technology selection.

The economic analysis (Class V) determined the profitability of the industrial magnetic separation plant, considering the national and international demand, initial investment, total operational cost, inflation rate, taxes, and net income.

The magnetic separation process designed and proposed in this study also includes returning the large particles and the non-magnetic material to the original extraction zone. Hence, the proposed design can be considered a non-destructive process, since the main extraction area will quickly recuperate its natural physical conditions, with the support of marine processes. Thus, considering the efficiency, economic feasibility, raw material availability, minimal environmental impact, and the wide range of Fe–Ti oxide applications, the proposed preliminary design demonstrates a capable industrial magnetic separation process.

**Supplementary Materials:** The following are available online: <https://www.mdpi.com/article/10.3390/resources11120121/s1>, Figure S1. Water content percentage in black sand samples from Ecuador. Figure S2. Granulometric curves of black sand samples from Ecuador. Table S1. Particle size (median size and mean size) obtained by DLS. Figure S3. Granulometric-derived parameters of sandy sediments in sampled areas in coastal Ecuador: coefficient of uniformity vs. median value. Table S2. Semi-quantitative chemical composition of sandy samples by SEM-EDS analysis expressed as oxides. Figure S4. Manual magnetic separation procedure: initial and final conditions.

**Author Contributions:** Conceptualization, W.T., J.C. and M.R.; methodology, W.T., D.V.-C., A.P.-C. and J.T.-Á.; validation, A.P.-C., J.T.-Á., A.V. and M.R.; formal analysis, W.T., J.C., A.P.-C., J.T.-Á. and M.R.; investigation, W.T., J.C., D.V.-C., A.P.-C., J.T.-Á. and M.R.; data curation, W.T., J.C. and D.V.-C.; writing—original draft preparation, W.T., J.C., A.P.-C., J.T.-Á. and M.R.; writing—review and editing, A.P.-C., J.T.-Á., A.V. and M.R.; visualization, W.T., A.V. and M.R.; supervision, A.P.-C. and M.R.; funding acquisition, A.V. and M.R. All authors have read and agreed to the published version of the manuscript.

**Funding:** This research was funded by SENESCYT, Ecuador (grant number PIC-18-INE-YACHAY-001) and Yachay Tech University (project CHEM21-10).

**Institutional Review Board Statement:** Not applicable.

**Data Availability Statement:** The data that support the findings of this study are available from the corresponding author (M.R.), upon reasonable request.

**Acknowledgments:** We thank José Manuel Fernández, Manuel Caetano, and Miguel Larrea from Yachay Tech University for their assistance during sampling trips and Marlon Chimarro for his assistance during the sieving analysis. We thank the National Institute of the Cultural Heritage (INPC) of Ecuador for its support in the SEM-EDS and DLS analysis.

**Conflicts of Interest:** The authors declare no conflict of interest.

## References

1. Hebatalrahman, A.; Zaki, S.; Younis, M. Black sands applications in construction and building. *Multi-Knowl. Electron Compr. J. Educ. Sci. Public* **2019**, *22*, 1–20.
2. Rodriguez, M.; Rosales, G.; Pinna, E.; Tunez, F.; Toro, N. Extraction of titanium from low-grade ore with different leaching agents in autoclave. *Metals* **2020**, *10*, 497. [[CrossRef](#)]
3. Yousef, L. Uranium adsorption using iron-titanium mixed oxides separated from ilmenite mineral, black sands, Rosetta, Egypt. *Arab J. Nucl. Sci. Appl.* **2017**, *50*, 43–57.
4. Pratesi, G. The 14 most Exotic Black Sand Beaches in the World. *U.S. News*, 8 March 2022.
5. Varner, K.; Rindfusz, K.; Gaglione, A.; Viveiros, E. *Nano Titanium Dioxide Environmental Matters: State of the Science Literature Review*; US Environmental Protection Agency: Washington, DC, USA, 2010.
6. Akinlabi, S.; Ogbonna, O.; Mashinini, P.; Adediran, A.; Fatoba, O.; Akinlabi, E. Titanium and epoxy for automobile application: A review. In Proceedings of the Eighth International Conference on Advances in Civil, Structural and Mechanical Engineering, Birmingham, UK, 23–24 April 2019.
7. Inestroza, J. *The Mineral Industry of Ecuador*; U.S. Geological Survey: Washington, DC, USA, 2021; pp. 201–208.
8. Ezhov, A.; Shvaljov, Y. Dry magnetic separation of iron ore of the bakchar deposit. *Procedia Chem.* **2015**, *15*, 160–166. [[CrossRef](#)]
9. Svoboda, J. *Magnetic Techniques for the Treatment of Materials*; Kluwer Academic Publishers: Dordrecht, The Netherlands, 2004; ISBN 1-4020-2038-4.
10. Baawuah, E.; Kelsey, C.; Addai-Mensah, J.; Skinner, W. A Novel Pneumatic Planar Magnetic Separator for Magnetite Beneficiation: A Focus on Flowsheet Configuration. *Minerals* **2020**, *10*, 759. [[CrossRef](#)]
11. Bikbov, M.; Karmazin, V.; Bikbov, A. Low-intensity magnetic separation: Principal stages of a separator development—what is the next step? *Phys. Sep. Sci. Eng.* **2004**, *13*, 53–67. [[CrossRef](#)]
12. Putro, A.; Lee, J. Analysis of longshore drift patterns on the littoral system of Nusa Dua Beach in Bali, Indonesia. *J. Mar. Sci. Eng.* **2020**, *8*, 749. [[CrossRef](#)]
13. Ridley, J. *Ore Deposit Geology*, 1st ed.; Cambridge University Press: Cambridge, UK, 2013.
14. Sayadi, A.; Lashgari, A.; Fouladgar, M.; Skibniewski, M. Estimating capital and operational costs of backhoe shovels. *J. Civ. Eng. Manag.* **2012**, *18*, 378–385. [[CrossRef](#)]
15. Kerkhof, P. Drying, growth towards a unit operation. *Dry. Technol.* **2001**, *19*, 1505–1541. [[CrossRef](#)]
16. Freire, F.; Vieira, G.; Freire, J.; Mujumdar, A. Trends in modeling and sensing approaches for drying control. *Dry. Technol.* **2014**, *32*, 1524–1532. [[CrossRef](#)]
17. Liu, K. Some factors affecting sieving performance and efficiency. *Powder Technol.* **2009**, *193*, 208–213. [[CrossRef](#)]
18. Abdel-Karim, A.; Moustafa, M.; El-Afandy, A.; Barakat, M. Mineralogy, Chemical Characteristics and Upgrading of Beach Ilmenite of the Top Meter of Black Sand Deposits of the Kafr Al-Sheikh Governorate, Northern Egypt. *Acta Geol. Sin.-Engl. Ed.* **2017**, *91*, 1326–1338. [[CrossRef](#)]
19. Cañas-Martínez, D.; Gauthier, G.; Pedraza-Avella, J. Photo-oxidative and photo-reductive capabilities of ilmenite-rich black sand concentrates using methyl orange as a probe molecule. *Photochem. Photobiol. Sci.* **2019**, *18*, 912–919. [[CrossRef](#)]
20. Cañas-Martínez, D.; Cipagauta-Díaz, S.; Manrique, M.; Gómez, R.; Pedraza-Avella, J. Photocatalytic hydrogen production using FeTiO<sub>3</sub> concentrates modified by high energy ball milling and the presence of Mg precursors. *Top. Catal.* **2021**, *64*, 2–16. [[CrossRef](#)]
21. Papadopoulos, A.; Lazaridis, S.; Kipourou-Panagiotou, A.; Kantiranis, N.; Koroneos, A.; Almpanakis, K. Mineralogy, Geochemistry and Provenance of Coastal Sands from Greece: New Insights on the REE Content of Black Coastal Sands from Aggelochori Area, N.-Greece. *Minerals* **2021**, *11*, 693. [[CrossRef](#)]
22. Satria, B.; Masrurah, Z.; Fajar, S. Magnetic susceptibility and grain size distribution as prospective tools for selective exploration and provenance study of iron sand deposits: A case study from Aceh, Indonesia. *Heliyon* **2021**, *7*, e08584. [[CrossRef](#)] [[PubMed](#)]
23. Mohammed, A.; Yunus, N.; Idris, M.; Najmi, N.; Jamal, Z.; Nomura, T. Phase transformations of Langkawi ilmenite ore during carbothermal reduction using palm char as renewable reductant. *Chem. Eng. Res. Des.* **2022**, *178*, 583–589. [[CrossRef](#)]
24. Khuzaima, N.; Rafezi, K.; Zaidi, N.; Hashim, M.; Rezan, S.A. Minerals Characterization of Magnetic and Non-Magnetic Element from Black Sand Langkawi. *Solid State Phenom.* **2018**, *280*, 440–447. [[CrossRef](#)]
25. Akser, M.; Pirkle, F.L.; Stratford, B.; Ipekoglu, B. Concentration and characterization of titanium minerals and zircon from the western Black Sea Coast sands of Turkey. *Min. Metall. Explor.* **1996**, *13*, 45–51. [[CrossRef](#)]
26. Rozendaal, A.; Philander, C.; Heyn, R. The coastal heavy mineral sand deposits of Africa. *S. Afr. J. Geol.* **2017**, *120*, 133–152. [[CrossRef](#)]
27. Diab, M.; Abu El Ghar, M.; Mohamed Gaafar, I.; Mohamed El Shafey, A.; Wageh Hussein, A.; Mohamed Fawzy, M. Potentiality of physical upgrading for valuable heavy minerals from Sermatai area, Egypt. *J. Min. Environ.* **2022**, *13*, 15–32. [[CrossRef](#)]

28. Abdel-Karim, A.; Zaid, S.; Moustafa, M.; Barakat, M. Mineralogy, chemistry and radioactivity of the heavy minerals in the black sands, along the northern coast of Egypt. *J. African Earth Sci.* **2016**, *123*, 10–20. [[CrossRef](#)]
29. Chen, L.; Xiong, D. Chapter Seven—Magnetic Techniques for Mineral Processing. In *Progress in Filtration and Separation*; Tarleton, S., Ed.; Academic Press, Elsevier Ltd.: London, OH, USA, 2015; pp. 287–324. [[CrossRef](#)]
30. Iranmanesh, M.; Hulliger, J. Magnetic separation: Its application in mining, waste purification, medicine, biochemistry and chemistry. *Chem. Soc. Rev.* **2017**, *46*, 5925–5934. [[CrossRef](#)] [[PubMed](#)]
31. Begum, N.; Norsaffirah, K.N.; Bari, M.F.; Rezan, S. Processing of Black Sand for the Recovery of Metal. *Mater. Sci. Forum* **2016**, *880*, 63–66. [[CrossRef](#)]
32. Wills, B.; Finch, J. Chapter 13—Magnetic and Electrical Separation. In *Wills' Mineral Processing Technology*; Butterworth-Heinemann: Oxford, UK, 2016; pp. 381–407. [[CrossRef](#)]
33. Arvidson, B.; Norrgran, D. Magnetic separation. In *Mineral Processing and Extractive Metallurgy—100 Years of Innovation*; Anderson, C., Dunne, R., Uhrig, J., Eds.; Society for Mining, Metallurgy and Exploration Inc.: Englewood, CO, USA, 2014; pp. 223–233.
34. Zong, Q.; Fu, L.; Bo, L. Variables and applications on dry magnetic separator. *E3S Web Conf.* **2018**, *53*, 02019. [[CrossRef](#)]
35. Shao, Y.; Veasey, T.; Rowson, N. Wet high intensity magnetic separation of iron minerals. *Magn. Electr. Sep.* **1996**, *8*, 41–51. [[CrossRef](#)]
36. Sánchez-Cortez, J. Conservation of geoh heritage in Ecuador: Situation and perspectives. *Int. J. Geoh heritage Park.* **2019**, *7*, 91–101. [[CrossRef](#)]
37. Toro-Álava, J. Enregistrement Des Surrections Liées aux Accrétions de Terrains Océaniques: Les Sédiments Crétacé–Paléogènes Des Andes d'Équateur. Ph.D. Thesis, Joseph Fourier University, Grenoble, France, 2007.
38. Lagos, K.; Marinkovic, B.; Dosen, A.; Guamán, M.; Guerrero, V.; Pardo, E.; Pontón, P. Data on phase and chemical compositions of black sands from “El Ostional” beach situated in Mompiche, Ecuador. *Data Brief* **2020**, *32*, 106214. [[CrossRef](#)]
39. Ludwig, H.-M.; Zhang, W. Research review of cement clinker chemistry. *Cem. Concr. Res.* **2015**, *78*, 24–37. [[CrossRef](#)]
40. Petroche, D.; Ramirez, A. The Environmental Profile of Clinker, Cement, and Concrete: A Life Cycle Perspective Study Based on Ecuadorian Data. *Buildings* **2022**, *12*, 311. [[CrossRef](#)]
41. MEM. *Plan Nacional de Desarrollo del Sector Minero 2020–2030*; Ministerio de Energía de Ecuador: Quito, Ecuador, 2020.
42. Primicias. *Recuperación del Sector Constructor Incentiva la Inversión Extranjera*; Primicias: Quito, Ecuador, 2021.
43. Carrasco, B.; Ávila, E.; Viloría, A.; Ricaurte, M. Shrinking-core model integrating to the fluid-dynamic analysis of fixed-bed adsorption towers for H<sub>2</sub>S removal from natural gas. *Energies* **2021**, *14*, 5576. [[CrossRef](#)]
44. Iglesias, I.; Jiménez, M.; Gallardo, A.; Ávila, E.; Morera, V.; Viloría, A.; Ricaurte, M.; Tafur, J.P. Mechanical properties and X-ray diffraction analyses of clay/sand pellets for CO<sub>2</sub> adsorption: The effects of sand content and humidity. *Oil Gas Sci. Technol.–Rev. D'ifp Energ. Nouv.* **2021**, *76*, 49. [[CrossRef](#)]
45. Sirirerkratana, K.; Kemacheevakul, P.; Chuangchote, S. Color removal from wastewater by photocatalytic process using titanium dioxide-coated glass, ceramic tile, and stainless steel sheets. *J. Clean. Prod.* **2019**, *215*, 123–130. [[CrossRef](#)]
46. AITE. *Boletín Mensual AITE*; Asociación de Industrias Textiles del Ecuador: Quito, Ecuador, 2016; p. 7.
47. CFN. *Ficha Sectorial: Prendas de Vestir*; Corporación Financiera Nacional: Quito, Ecuador, 2021.
48. Ricaurte, M.; Ordóñez, P.; Navas-Cárdenas, C.; Meneses, M.; Tafur, J.; Viloría, A. Industrial Processes Online Teaching: A Good Practice for Undergraduate Engineering Students in Times of COVID-19. *Sustainability* **2022**, *14*, 4776. [[CrossRef](#)]
49. Boggs, S. *Principles of Sedimentology and Stratigraphy*, 4th ed.; Pearson Prentice Hall: Upper Saddle River, NJ, USA, 2006; ISBN 0-13-154728-3.
50. Kursun, I.; Ozkan, S.; Terzi, M.; Tombal, T. *Geotechnical Engineering and Soil Testing*, 1st ed.; Oxford University Press: New York, NY, USA, 1992; ISBN 0-19-510719-5.
51. Kursun, I.; Ozkan, S.; Terzi, M.; Tombal, T. Determination of particle size distribution of quartz sands by novel methods: A case study. In Proceedings of the 6th International Conference on Computer Applications in the Minerals Industries, Istanbul, Turkey, 5–7 October 2016; pp. 5–7.
52. Wu, Z.; Hu, Y.; Lee, D.; Mujumdar, A.; Li, Z. Dewatering and drying in mineral processing industry: Potential for innovation. *Dry. Technol.* **2010**, *28*, 834–842. [[CrossRef](#)]
53. Green, D.; Perry, R. *Perry's Chemical Engineers' Handbook*, 8th ed.; McGraw-Hill Professionals: New York, NY, USA, 2008.
54. Delele, M.A.; Weigler, F.; Mellmann, J. Advances in the application of a rotary dryer for drying of agricultural products: A review. *Dry. Technol.* **2015**, *33*, 541–558. [[CrossRef](#)]
55. Fernandes, N.; Ataíde, C.; Barrozo, M. Modeling and experimental study of hydrodynamic and drying characteristics of an industrial rotary dryer. *Braz. J. Chem. Eng.* **2009**, *26*, 331–341. [[CrossRef](#)]
56. Couper, J.; Penny, W.; Walas, S. *Chemical Process Equipment Selection and Design*, 3rd ed.; Butterworth-Heinemann: Waltham, MA, USA, 2012.
57. Wang, G.; Tong, X. Screening efficiency and screen length of a linear vibrating screen using DEM 3D simulation. *Min. Sci. Technol.* **2011**, *21*, 451–455. [[CrossRef](#)]
58. Goyal, S.; Jogdand, S.; Agrawal, A. Energy use pattern in rice milling industries—A critical appraisal. *J. Food Sci. Technol.* **2014**, *51*, 2907–2916. [[CrossRef](#)] [[PubMed](#)]

59. Tripathy, S.; Banerjee, P.; Suresh, N. Effect of desliming on the magnetic separation of low-grade ferruginous manganese ore. *Int. J. Miner. Metall. Mater.* **2015**, *22*, 661–673. [[CrossRef](#)]
60. Dobbins, M.; Dunn, P.; Sherrell, I. Recent advances in magnetic separator designs and applications. In Proceedings of the 7th International Heavy Minerals Conference, Johannesburg, South Afrika, 20–23 September 2009.
61. Jassim, H.; Lu, W.; Olofsson, T. Predicting energy consumption and CO<sub>2</sub> emissions of excavators in earthwork operations: An artificial neural network model. *Sustainability* **2017**, *9*, 1257. [[CrossRef](#)]
62. Gavriletea, M. Environmental impacts of sand exploitation. Analysis of sand market. *Sustainability* **2017**, *9*, 1118. [[CrossRef](#)]
63. Rukmana, D.; Salman, D.; Alimuddin, I. Arsyad Economic and environmental impacts of sand mining activities at sadang river Pinrang Regency, South Sulawesi. *IOP Conf. Ser. Earth Environ. Sci.* **2020**, *575*, 012043. [[CrossRef](#)]
64. Alarcón, I. La extracción de arena de Playas y ríos se incrementó. *El Comercio*, 8 June 2019.
65. Fu, Z. The mechanism of imported iron ore price in China. *Mod. Econ.* **2018**, *9*, 1908–1931. [[CrossRef](#)]
66. Shatokha, V. *Iron Ores and Iron Oxide Materials*, 1st ed.; Shatokha, V., Ed.; IntechOpen: New Delhi, India, 2018; ISBN 978-1-78923-320-9.
67. Yanchapaxi, L. *The Export Supply of Ferrotitaniferous Sand and Its Prospects for Export to the Shanghai Market, Case of the Company Minagrotec, Ecuador*; 2015 Export Plan; Universidad Tecnológica Equinoccial: Quito, Ecuador, 2016.
68. Towler, G.; Sinnott, R. *Chemical Engineering Design Principles, Practice and Economics of Plant and Process Design*, 2nd ed.; Butterworth-Heinemann Press: Oxford, UK, 2013; ISBN 9780080966595.
69. Brown, T. *Engineering Economics and Economic Design for Process Engineers*, 1st ed.; CRC Press: Boca Raton, FL, USA, 2016; ISBN 9780429127090.